AD-A115 717 NAVAL POSTGRADUATE SCHOOL MONTEREY CA F/G 8/7
THE IMPACT OF TECTONIC ACTIVITY IN THE DEVELOPMENT OF MONTEREY --ETC(U)
MAR 82 R L ALLEN

UNCLASSIFIED

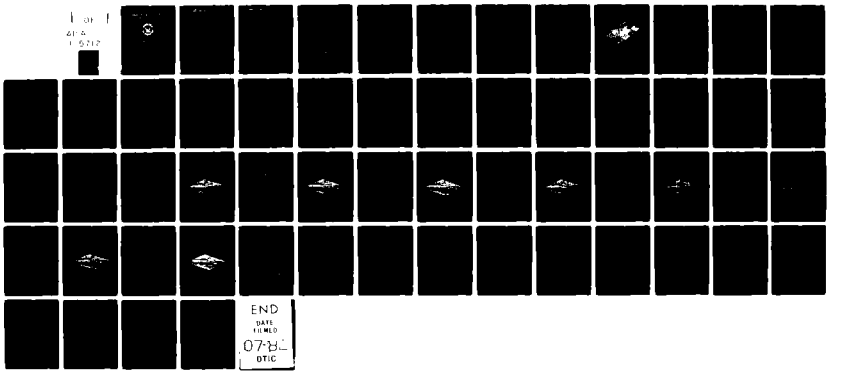

END
DATE FILMED
07-82
DTIC

(2)

NAVAL POSTGRADUATE SCHOOL
Monterey, California

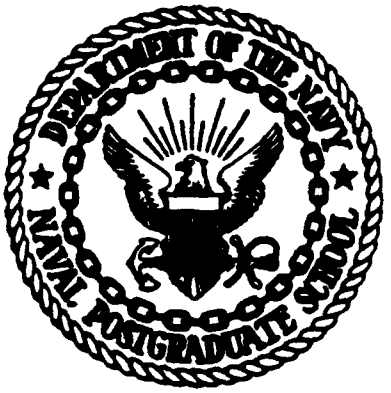

THESIS

THE IMPACT OF TECTONIC ACTIVITY
IN THE DEVELOPMENT OF MONTEREY
SUBMARINE CANYON

by

Robert Lloyd Allen, Jr.

March 1982

Thesis Advisors: E. C. Haderlie
H. G. Greene

Approved for public release; distribution unlimited.

UNCLASSIFIED

SECURITY CLASSIFICATION OF THIS PAGE (When Data Entered)

REPORT DOCUMENTATION PAGE		READ INSTRUCTIONS BEFORE COMPLETING FORM
1. REPORT NUMBER	2. GOVT ACCESSION NO. AD-A115 717	3. RECIPIENT'S CATALOG NUMBER
4. TITLE (and Subtitle) The Impact of Tectonic Activity in the Development of Monterey Submarine Canyon		5. TYPE OF REPORT & PERIOD COVERED Master's Thesis; March 1982
		6. PERFORMING ORG. REPORT NUMBER
7. AUTHOR(s) Robert Lloyd Allen, Jr.		8. CONTRACT OR GRANT NUMBER(s)
9. PERFORMING ORGANIZATION NAME AND ADDRESS Naval Postgraduate School Monterey, California 93940		10. PROGRAM ELEMENT, PROJECT, TASK AREA & WORK UNIT NUMBERS
11. CONTROLLING OFFICE NAME AND ADDRESS Naval Postgraduate School Monterey, California 93940		12. REPORT DATE March 1982
		13. NUMBER OF PAGES 57
14. MONITORING AGENCY NAME & ADDRESS (if different from Controlling Office)		15. SECURITY CLASS. (of this report) Unclassified
		15a. DECLASSIFICATION/DOWNGRADING SCHEDULE

16. DISTRIBUTION STATEMENT (of this Report)

Approved for public release; distribution unlimited.

17. DISTRIBUTION STATEMENT (of the abstract entered in Block 20, if different from Report)

18. SUPPLEMENTARY NOTES

19. KEY WORDS (Continue on reverse side if necessary and identify by block number)

Monterey Submarine Canyon
submarine canyon
tectonics

20. ABSTRACT (Continue on reverse side if necessary and identify by block number)

Evidence is presented that indicates that Monterey Submarine Canyon was once the terminus of a major land drainage system. This pre-existing drainage system is not in evidence today because it has been altered by displacement along the San Andreas Fault. A numerical model based on conservation of mass and plate tectonic reconstruction is utilized to reconstruct the topography of the region as it

DD FORM 1 JAN 73 1473 EDITION OF 1 NOV 65 IS OBSOLETE S/N 0102-014-6601

UNCLASSIFIED

SECURITY CLASSIFICATION OF THIS PAGE (When Data Entered)

(20. ABSTRACT Continued)

appeared prior to onset of motion along the San Andreas Fault. Model results indicate that the Colorado River may have drained into Monterey Bay during early Miocene time.

Approved for public release; distribution unlimited

The Impact of Tectonic Activity in the Development of Monterey Submarine Canyon

by

Robert Lloyd Allen, Jr.
Lieutenant, United States Navy
B. S., Florida State University, 1975

Submitted in partial fulfillment of the
requirements for the degree of

MASTER OF SCIENCE IN METEOROLOGY AND OCEANOGRAPHY

from the

NAVAL POSTGRADUATE SCHOOL

March, 1982

Author: R. L. Allen Jr.

Approved by: E. B. Kraitzik
Thesis Advisor

Co-Advisor

Chairman, Department of Oceanography

William M. Tolles
Dean of Science and Engineering

ABSTRACT

Evidence is presented that indicates that Monterey Submarine Canyon was once the terminus of a major land drainage system. This pre-existing drainage system is not in evidence today because it has been altered by displacement along the San Andreas Fault. A numerical model based on conservation of mass and plate tectonic reconstructions is utilized to reconstruct the topography of the region as it appeared prior to onset of motion along the San Andreas Fault. Model results indicate that the Colorado River may have drained into Monterey Bay during early Miocene time.

TABLE OF CONTENTS

ACKNOWLEDGMENTS

This study would not have been possible without the efforts of my co-advisors; Dist. Prof. E. C. Haderlie of the Naval Postgraduate School and Dr. H. G. Greene of the U. S. Geological Survey.

Dr. Haderlie's support and guidance were the lifeblood of this thesis during the early going. His unparalleled scientific curiosity and foresight literally made this study possible.

Dr. Greene agreed to co-advise in spite of a heavy work load with the U. S. Geological Survey. I was indeed fortunate to have the foremost authority on the geology of Monterey Bay as a co-advisor.

Two very capable members of the NPS Meteorology Department provided valuable assistance. Prof. R. T. Williams was very helpful with model design and trouble-shooting suggestions. P. W. Phoebus, an outstanding programmer, provided much needed technical assistance in programming.

Most of all, I would like to thank my wife, Teresa, who shared in all the ups and downs from beginning to end, and who is a constant source of inspiration to me.

I. INTRODUCTION

Monterey Submarine Canyon is the largest of the California submarine canyons. Traced seaward from its head near Elkhorn Slough in Monterey Bay, the canyon axis follows a meandering path for approximately 100 km before emerging as a fan valley at a depth of about 3 km (Figure 1). From this point, the fan valley can be traced for another 400 km across the Monterey deep-sea fan. The volumes of the canyon and the fan have been estimated to be 450 km^3 and 30,000 km^3 respectively (Menard, 1960). The walls of the canyon are approximately 1,500 m high at one point, producing relief comparable to that of the Grand Canyon of the Colorado River (Figure 2).

Such is the magnitude of this feature that two of its tributaries have been named. Carmel Canyon branches south and heads very close to shore off Monastery Beach in Carmel Bay. Soquel Canyon branches northward near the canyon head and extends toward the town of Soquel, east of Santa Cruz.

The major canyon axis follows a fault contact near the head and is flanked by Tertiary sediments on both sides. At its outer limits; beyond about 20 km from its head at Elkhorn Slough, there is no indication of faulting along the canyon axis and the canyon course is purely erosional (Greene, 1977). Soquel Canyon is cut entirely in poorly indurated seimentary strata, while Carmel Canyon is eroded in granodiorite on the east and highly indurated sedimentary rocks on the west.

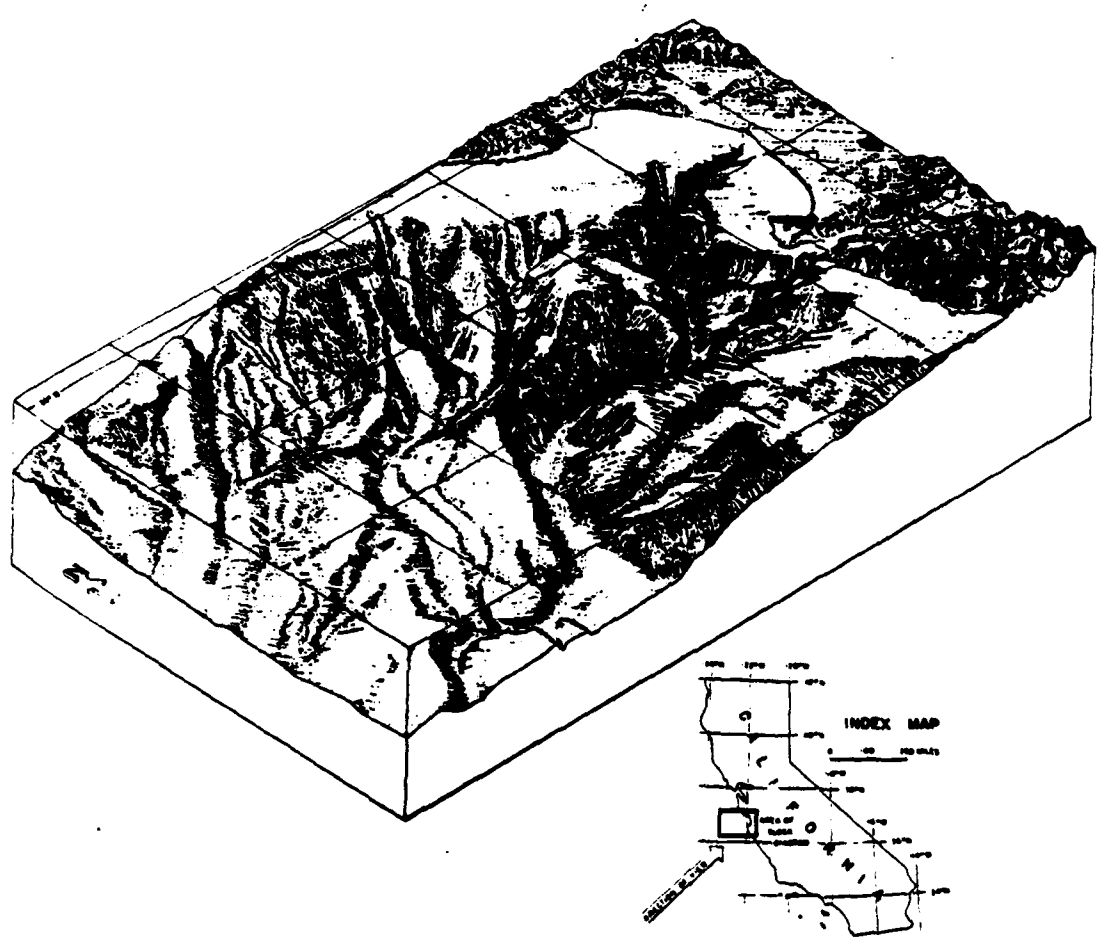

Figure 1. The Monterey and Carmel Submarine Canyons off the central California Coast. (Diagram by Tau Rho Alpha, USGS)

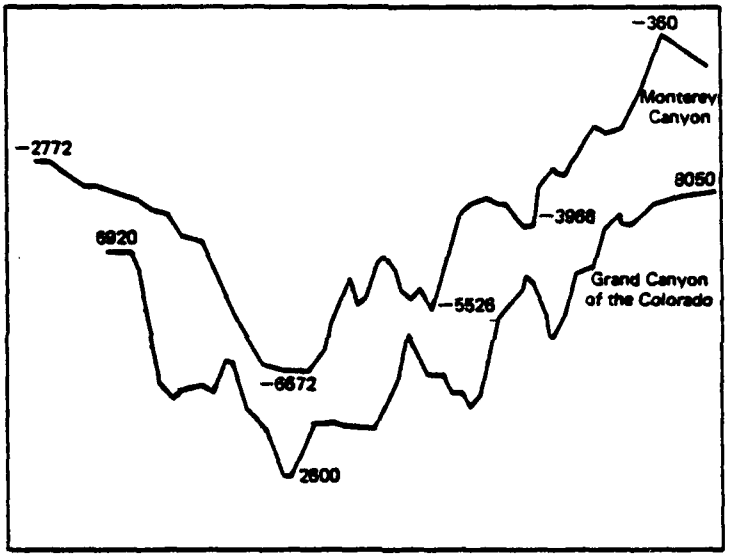

Figure 2. A comparison of the profiles of the Grand Canyon of the Colorado River and the Monterey Submarine Canyon, showing them to have similar relief. Elevations relative to sea level are given in feet. Vertical exaggeration is 5X. (After F. P. Shepard, Submarine Geology, 3rd Ed., Harper and Row, 1973.)

Like many of the submarine canyons along the California coast, Monterey Canyon does not lie seaward of a large land drainage system. The Salinas River is the largest of several small rivers which drain into Monterey Bay, all of which appear diminutive in comparison with Monterey Canyon. An explanation of this enigma was proposed by Martin and Emery (1967) when they suggested that Monterey Canyon had received drainage from the Great Valley of California, through the San Francisco Bay region during late Miocene, Pliocene and early Pleistocene time. Although some questions were answered by this hypothesis, others remain unanswered. Martin and Emery noted that the amount of material in Monterey Fan could not have resulted from the Great Valley connection which they proposed. In addition, they noted the existence of buried erosional features which led them to conclude that Monterey Canyon is a re-excavation of a pre-existing submarine canyon. As Martin and Emery noted, these buried erosional features, Elkhorn Erosion Surface and Pajaro Gorge, pre-dated their Great Valley Connection. The age and size of this pre-existing canyon were established by Greene (1977) using seismic profiling techniques. Greene's profiles confirm the fact that this pre-existing canyon existed prior to early Miocene time and is still not entirely re-excavated in some areas (Figure 3). Greene's evidence indicates that the lower reaches of Monterey Canyon have been displaced northward and are represented today by Pioneer and Ascension Canyons. According to Greene's theory,

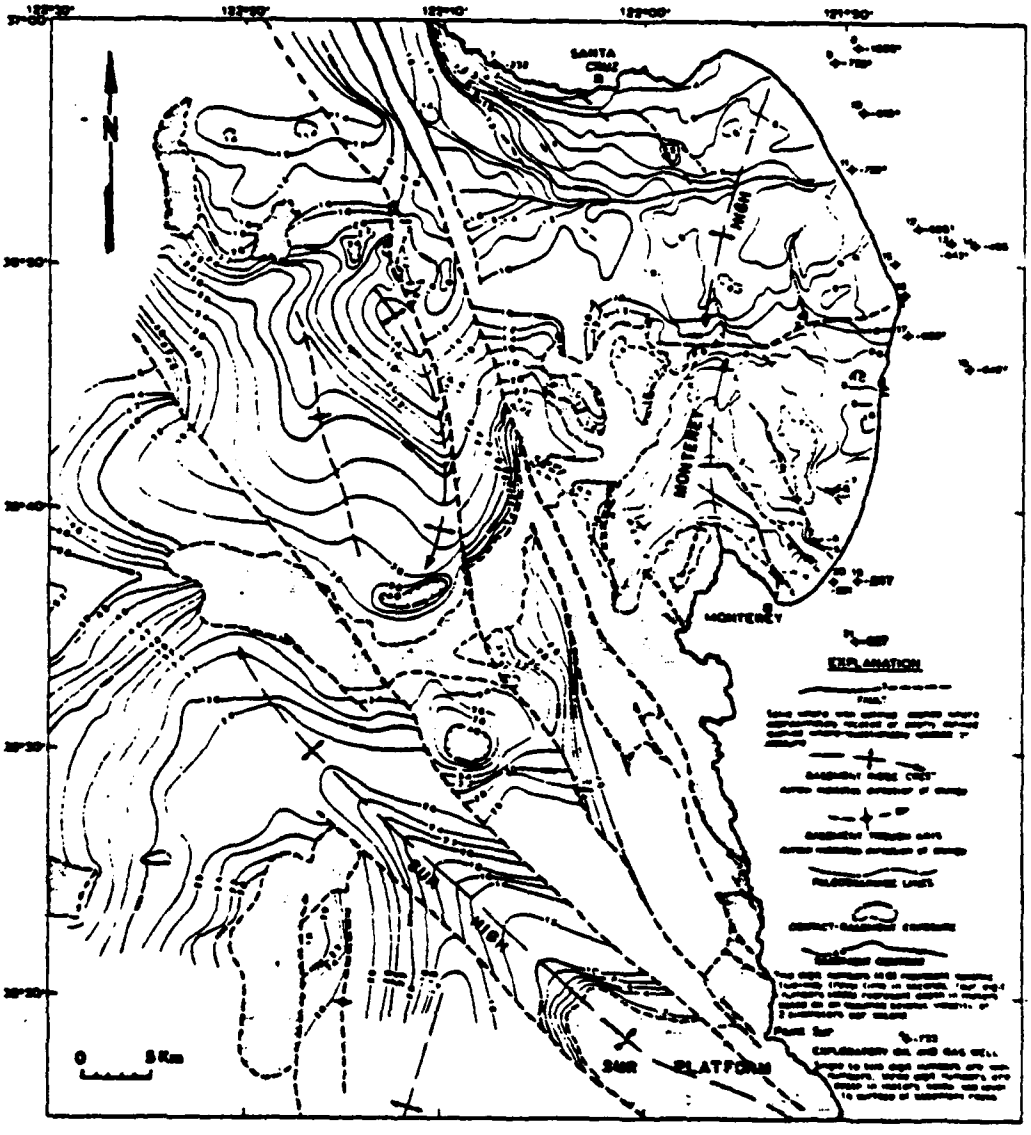

Figure 3. Basement contour map Monterey Bay Region, California (from Greene, 1977)

displacements along the Palo Colorado-San Gregorio Fault and the Ascension Fault over the past 20 million years may have moved these canyons into their present positions.

Although it is presently one of the largest submarine canyons in the world, there is evidence to indicate that Monterey Canyon is an incomplete re-excavation of a larger canyon. The mechanism involved in excavation of this earlier canyon and creation of Monterey Fan is unknown.

One possible explanation is that Monterey Canyon was the terminus of a large land drainage system which existed in pre-early Miocene time. Large scale deformation of topography since early Miocene has removed the canyon from its source and produced changes in the drainage patterns of the area (Clark and Rietman, 1973; Greene, 1977; Martin and Emery, 1967; Starke and Howard, 1968).

The topographic changes which have occurred since early Miocene along the west coast of North America have been extensive. About 30 million years ago, during Oligocene time, the East Pacific Rise came in contact with the North American Plate. Relative motion between the Pacific and North American plates came to be expressed along right lateral strike-slip faults on the continental margin. During early Miocene time, the zone of strike-slip faulting between the Pacific and North American Plates shifted inland to the San Andreas Fault. Since its inception, approximately 300 km of right slip has occurred along the San Andreas Fault (Crowell, 1962).

Such large-scale motion would undoubtedly have had great impact on any pre-existing drainage system. Reconstruction of topography as it existed prior to the onset of motion on the San Andreas Fault is difficult. Motion along the fault has not been constant in either speed or azimuth over this interval. In addition, compressional forces along the fault have uplifted areas resulting in the creation of new topographic features (Greene, 1977).

Due to the complexity of the problem, a numerical model is utilized to reconstruct the topography of the area as it appeared in early Miocene time. The model simply reverses motion along the San Andreas Fault utilizing data from plate tectonic reconstructions and imposing mass conservation. It does not reverse the effects of erosion or deposition, motion along other faults, or any other forces. However, since motion along the San Andreas Fault has contributed greatly to the alteration of topography since the early Miocene, results from such a model may be expected to provide useful insights into early Miocene topography.

II. PROCEDURE

The model was designed to simulate a reversal of the motion which has occurred along the San Andreas Fault over the past 21 million years. In simulating this reversal, mass must be conserved. The conservation of mass states that:

$$\frac{dm}{dt} = \frac{\partial m}{\partial t} + \vec{v} \cdot \vec{\nabla} m + m\vec{\nabla} \cdot \vec{v} = 0, \qquad (1)$$

where

m = mass,

t = time, and

$\vec{v}$ = velocity.

In other words, the total change in mass is equal to the local time change plus mass flux divergence. Since the total change is zero, mass is conserved and the local change must balance transport:

$$\frac{\partial m}{\partial t} = - \vec{v} \cdot \vec{\nabla} m - m\vec{\nabla} \cdot \vec{v}. \qquad (2)$$

Since total mass equals mass density (ρ) times total volume (V), then:

$$\frac{\partial (\rho V)}{\partial t} = - \vec{v} \cdot \vec{\nabla} (\rho V) - \rho V \vec{\nabla} \cdot \vec{v} \qquad (3)$$

If we assume that density is constant in space and time, it can be eliminated:

$$\frac{\partial V}{\partial t} = - \vec{v} \cdot \vec{\nabla} V - V \vec{\nabla} \cdot \vec{v} \qquad (4)$$

Finally, when dealing with a unit area, volume is expressed in height above/below sea level (h) (Equation (5).

$$\frac{\partial h}{\partial t} = - \vec{v} \cdot \vec{\nabla} h - h \vec{\nabla} \cdot \vec{v} \qquad (5)$$

From Equation (5), with an initial height field and a velocity field, topographic changes in time may be predicted.

The height field is a 70 x 64 array of topographic and bathymetric heights as illustrated in Figure 4. The grid interval is 10 minutes of longitude in the x direction and 10 minutes of latitude in the y direction (15.2 and 18.5 km, respectively). This interval in the x direction corresponds to true grid spacing at 35 degrees north, and introduces a departure from a spherical earth of approximately 7% at the northern and southern extremes.

While the height field simply provides initialization for the model, the velocity field defines the fault and drives the model. As illustrated in the initial velocity field (Figure 5), the portion of the grid which lies to the east of the San Andreas Fault is held fixed while that portion to the west of the fault is moved southeastward. Along the fault

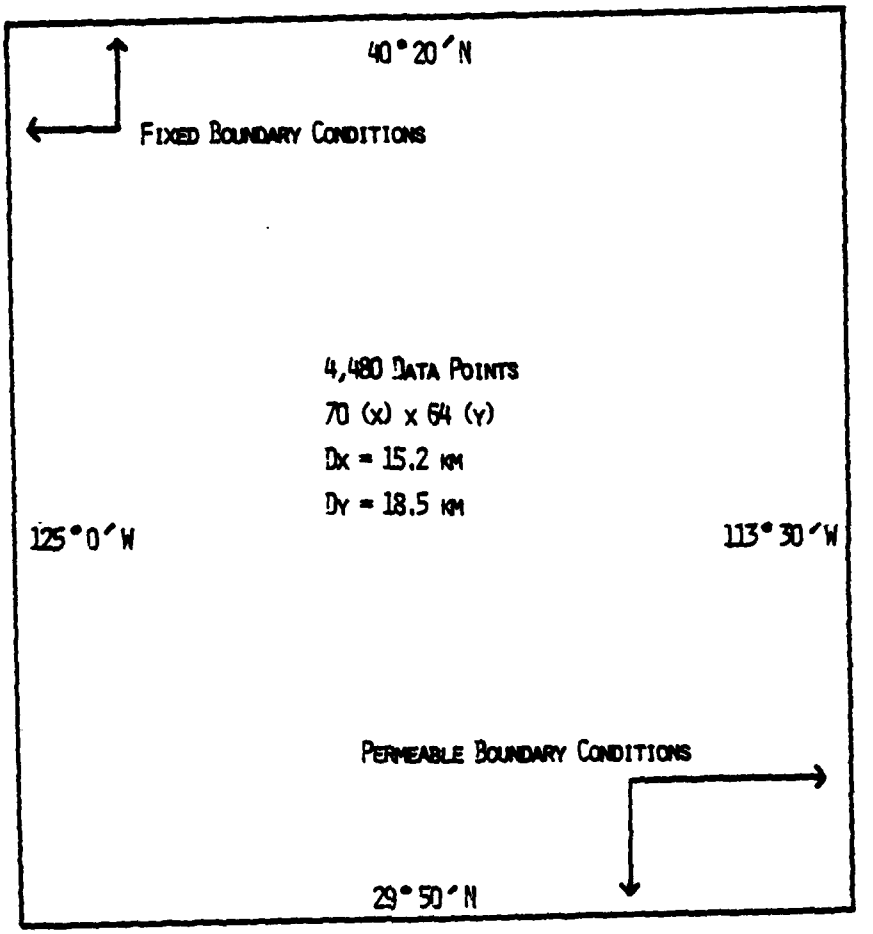

Figure 4. Grid features

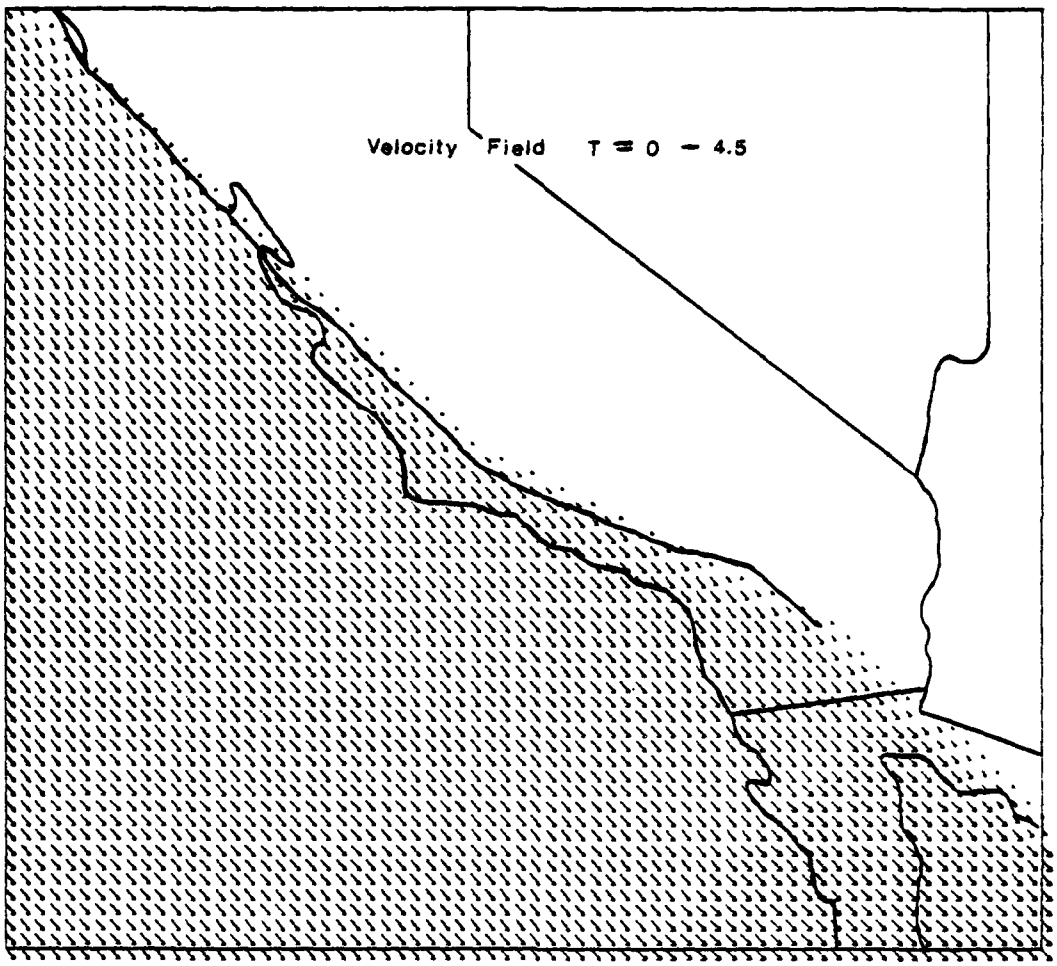

Figure 5. Velocity field: 0-4.5 million years before present, vectors indicate direction and relative magnitude of velocity at each point.

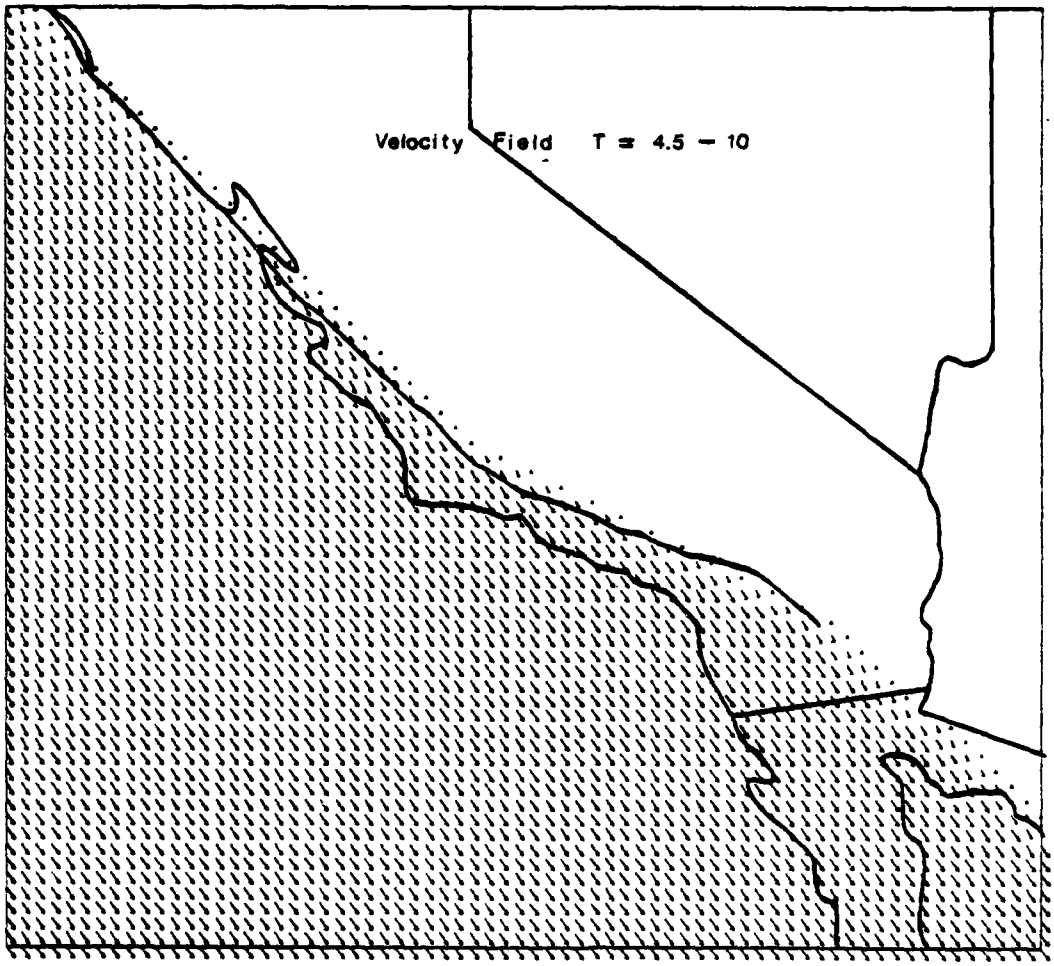

Figure 6. Velocity field: 4.5-10 million years before present, vectors indicate direction and relative magnitude of velocity at each point.

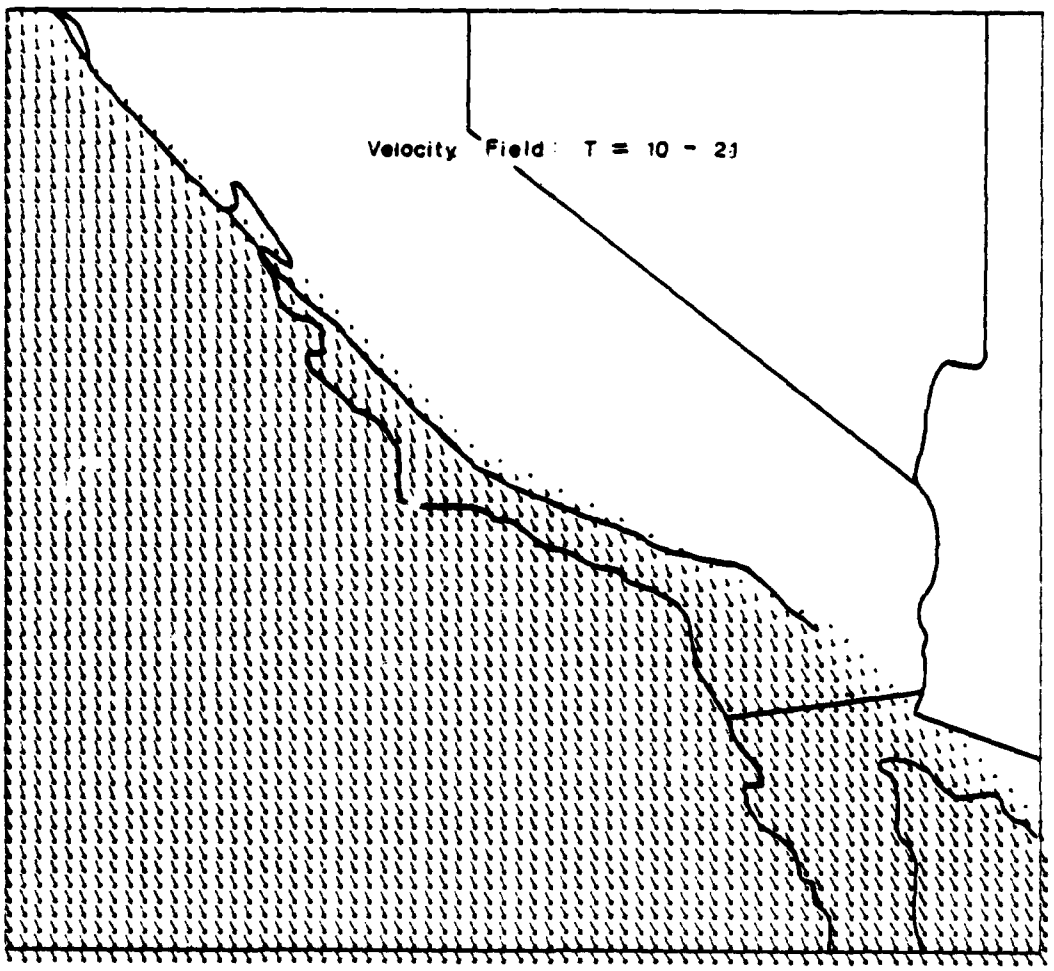

Figure 7. Velocity field: 10-21 million years before present, vectors indicate direction and relative magnitude of velocity at each point.

itself, there is a gradation of the velocity field as depicted in Figure 8. At the position of the fault, the magnitude of the velocity field is reduced by one-half. At the next grid point to the east, the velocity is one-quarter as large as it is in the moving block. At the first grid point to the west of the fault, velocity is three-quarters as large as the velocity of the moving block. This configuration results in a zone of velocity gradation across the fault and prevents the numerical instabilities which may arise from modelling the fault as a more severe velocity discontinuity. Previous attempts without a gradation of velocity across the fault resulted in unreasonable topography. The components of the velocity field, speed and direction, will be discussed separately.

Directions were derived from an algorithm which generates smooth fields to match directions at three points where directions are known from plate tectonic reconstructions (Silver et al., unpub. data). Directions of relative motion between the North American and Pacific Plates relative to three points on the North American Plate during three time intervals are presented in Table I. Corresponding values from the model algorithm are displayed in parentheses for comparison. Since the model simulates a reversal of motion, all directions are reduced by 180° to produce the velocity fields depicted in Figures 5-7. These figures illustrate the velocity fields used at different times in the model. The vectors to the left

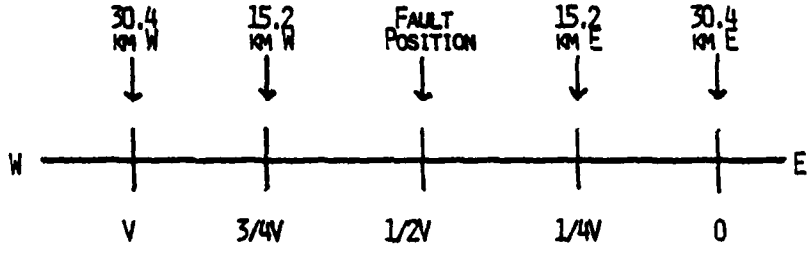

Figure 8. Velocity gradient along the fault

TABLE I
(From Blake et al., 1978)

Azimuth of Average Movement Direction of Pacific Plate Relative to Points on North American Plate

Values from model algorithms in parenthesis

Age (my)	36°N, 121.5°W	33°N, 119°W	26°N, 112°W
0--4.5	321.2° (321.2°)	318.6° (318.5°)	311.7° (311.7°)
4.5--10	328.0° (328.0°)	325.7° (325.6°)	319.5° (319.5°)
10--21.2	339.0° (339.2°)	335.0° (334.9°)	323.9° (324.0°)

side of the figures represent the moving block. It can be seen that there is a very slight change in the direction from one end of the field to the other in all three figures as would be expected from Table I. On the right side of each figure is an area with no vectors. This is the stationary portion of the grid. The shorter vectors at the intersection of the stationary block and the moving block represents the fault zone. As previously discussed, there is a gradient in the magnitudes of the velocities across the fault. This is reflected in the comparatively shorter vectors in the fault zone. The actual position of the San Andreas Fault is superimposed on these figures for comparison. It can be seen from Figures 5-7 and from the values in Table I that the motion changes with time to a more westerly direction becoming less compressional and more nearly aligned with the fault axis.

Speeds were derived from a combination of sources. Plate tectonic reconstruction (Atwater, 1973) produces an accelerating

velocity field which would have resulted in approximately 610 km of offset if all motion had been expressed as fault displacement. How much of this displacement is actually expressed in offsets along the San Andreas and other faults is unclear. Evidence for a 260 km offset along the San Andreas Fault (Crowell, 1962) establishes a conservative estimate and is the reference displacement utilized in this model. Although displacements from plate tectonic reconstruction do not match displacements derived from geologic evidence, the acceleration of motion between two plates, as derived from plate tectonic reconstruction, is not disputed by geologic evidence (Atwater, 1973). This acceleration of motion is incorporated into the model by reducing velocities from plate tectonic reconstruction such that the total resultant offset equals 260 km. This is accomplished by multiplying the velocities by a scaling factor, s = 260 km/610 km = .426. Resultant scaled velocities as well as original velocities derived from plate tectonic reconstruction (Atwater, 1973) are listed in Table II.

TABLE II

Time Period (Million years before present)	Relative Motion Pacific/N. American Plates	Relative Motion San Andreas Fault
21--10	1.3 cm/yr	0.6 cm/yr
10--4.5	4.0 cm/yr	1.7 cm/yr
4.5--	5.5 cm/yr	2.3 cm/yr

The height and velocity fields are substituted into the Continuity Equation (Equation (5)) using finite differencing schemes. In discussing differencing schemes, the following coordinate system and symbology will be used:

$H_{(i,j,t)}$ = reference point, height at a location on a horizontal plane identified by coordinates i (east) and j (north) at time t

u = velocity component in the i (east) direction

v = velocity component in the j (north) direction

Δt = interval of time (200,000 years in this model)

Δx = interval of space on the i axis. For example, the distance between $H_{(i,j,t)}$ and $H_{(i+1,j,t)}$

Δy = interval of space on the j axis. The distance between $H_{(i,j,t)}$ and $H_{(i,j+1,t)}$

The primary centered differencing scheme used in this model expresses Equation (5) in the following way:

$$\frac{H(i,j,t+1) - H(i,j,t-1)}{2\Delta t} = \frac{-u(i,j,t)[H(i+1,j,t)-H(i-1,j,t)]}{2\Delta x} - \frac{v(i,j,t)[H(i,j+1,t)-H(i,j-1,t)]}{2\Delta y} - \frac{H(i,j,t)[u(i+1,j,t)-u(i-1,j,t)]}{2\Delta x} - \frac{H(i,j,t)[v(i,j+1,t)-v(i,j-1,t)]}{2\Delta y} \quad (6)$$

This scheme is centered in space and time. It can not be used initially since it requires height fields at two different times (t and t-1) in order to predict the height at t+1. In addition, it can't be used on the grid boundaries since it would require the input of values beyond the range of the data field. However, it offers the advantage of centered differencing and favorable numerical stability.

Forward differencing must be used to predict the height fields on the first iteration for subsequent input into the primary centered scheme. Using forward time and centered space differencing,

$$\frac{H(i,j,t+1)-H(i,j,t)}{\Delta t} = - \frac{u(i,j,t)[H(i+1,j,t)-H(i-1,j,t)]}{2\Delta x} - \frac{v(i,j,t)[H(i,j+1,t)-H(i,j-1,t)]}{2\Delta y} - \frac{H(i,j,t)[u(i+1,j,t)-u(i-1,j,t)]}{2\Delta x} - \frac{H(i,j,t)[v(i,j+1,t)-v(i,j-1,t)]}{2\Delta y} \quad (7)$$

As with all numerical methods, numerical stability is an important consideration and limits the size of the time step (Δt) to be utilized. The Courant-Friedrichs-Levy (CFL) condition (Courant et al., 1928) for computational stability (Equation (8)) applies for this model.

$$\left|\frac{V\ \Delta t}{\Delta x}\right| \leq 1 \quad (8)$$

It controls the size of the time step (Δt) and grid spacing ($\Delta x, \Delta y$) such that motion does not cover more than one grid space between computations. With this model, Δt must be less than or equal to 500,000 years. The time step used is 200,000 years.

Boundary conditions are illustrated in Figure 4. As previously discussed, centered space differencing can not be used on the perimeters of the grid. Two different types of boundary conditions are used in this model. Boundaries in the direction of motion of the moving block (the eastern and southern boundaries) must be permeable. For this reason, the Upstream Differencing scheme (Haltiner and Williams, 1980, p. 130) is used on these boundaries. This scheme produces a permeable boundary where it intersects the moving block and establishes a rigid boundary condition for the stationary block:

$$\frac{H(i,j,t+1)-H(i,j,t)}{\Delta t} = - \frac{u(i-1,j,t)[H(i,j,t)-H(i-1,j,t)]}{\Delta x} - \frac{H(i-1,j,t)[u(i,j,t)-u(i-1,j,t)]}{\Delta x} \quad (8)$$

Fixed boundary conditions are imposed on the northern and western boundaries. Maintaining the points on these boundaries at their initial heights introduces errors where these points lie on the moving portion of the grid. As topography on these boundaries moves toward the interior of the grid, a false field is created in their previous

positions. Resultant erroneous values are eliminated from output by moving the northern and western boundaries inward (for display only) such that the northwest corner of the grid maintains its position relative to the moving block. This is illustrated in Figure 9.

The model produces output at 3 million year intervals. Output is displayed in a three dimensional form as well as a contoured plan view at each interval (Figures 10-25). The three dimensional computer graphics simulate viewing the terrain from a vantage point at high elevation over the Pacific Ocean looking northeast. Submarine bathymetry is included and all vertical heights are exaggerated by a factor of 15.

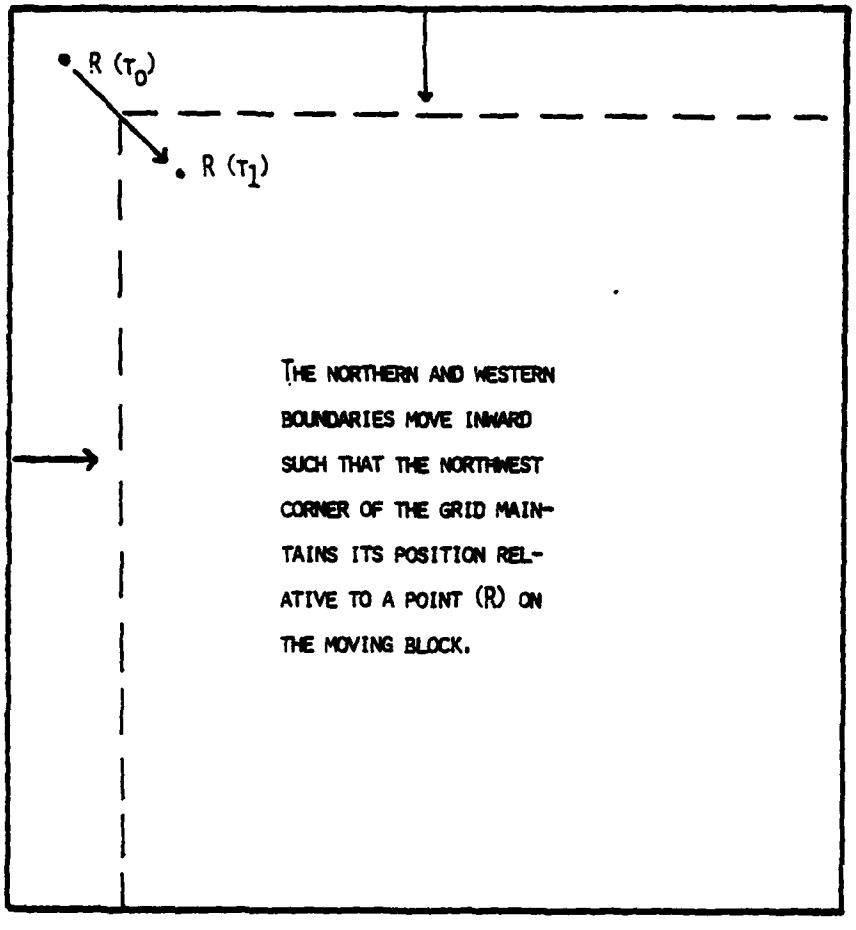

Figure 9. Movement of boundaries for display

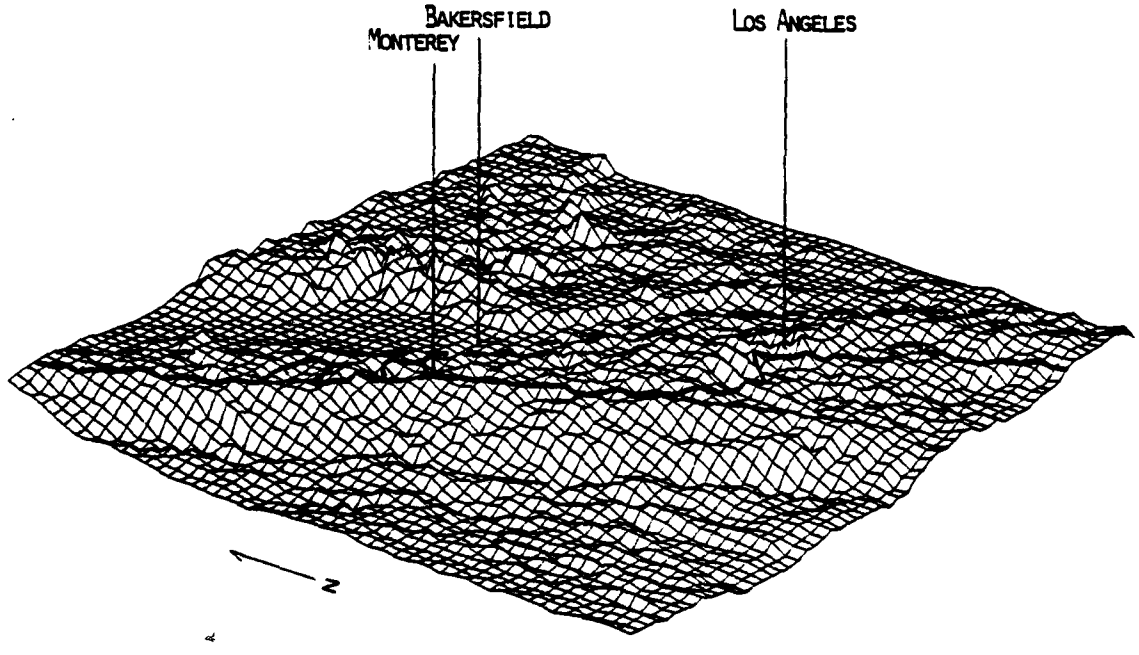

Figure 10. Topography 21 million years before present

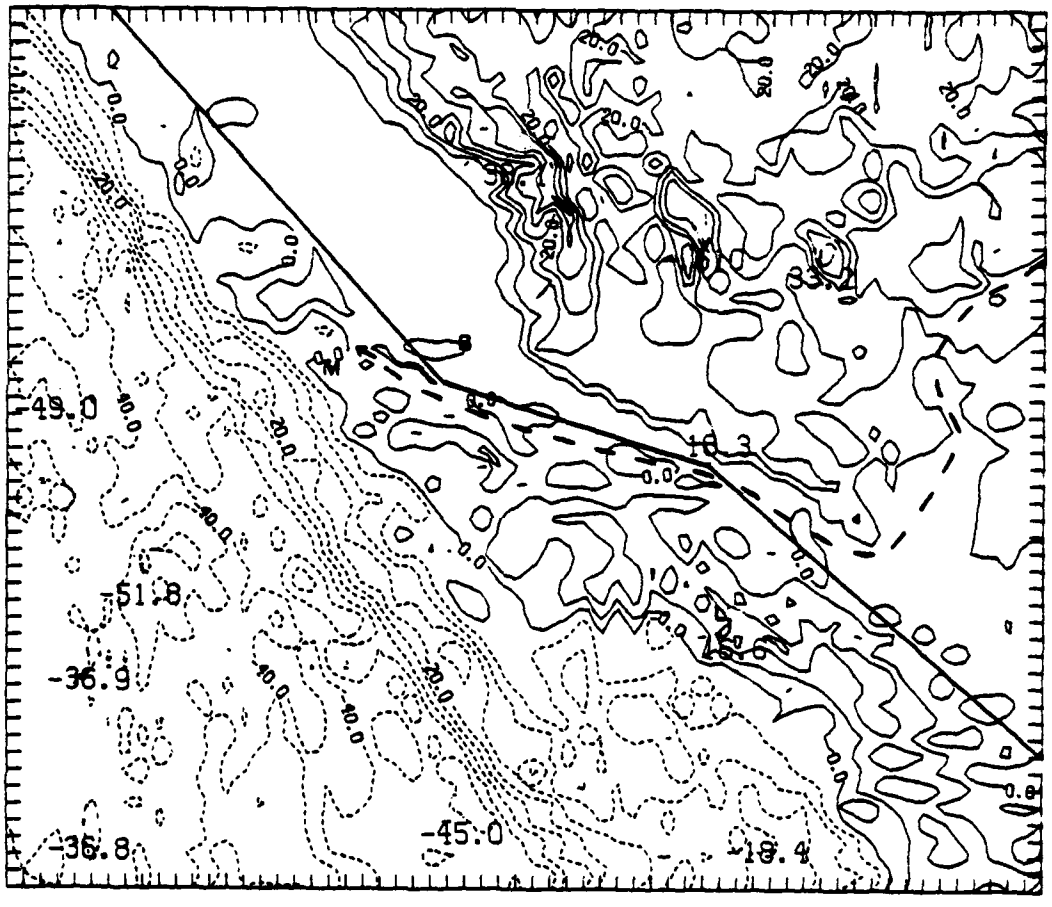

Figure 11. Twenty-one million years before present. On all contour plots; contour interval = 500 m, figures in hundreds of meters, bathymetry in dashed lines, inferred drainage is heavy dashed line, M, B, and L represent Monterey, Bakersfield and Los Angeles respectively

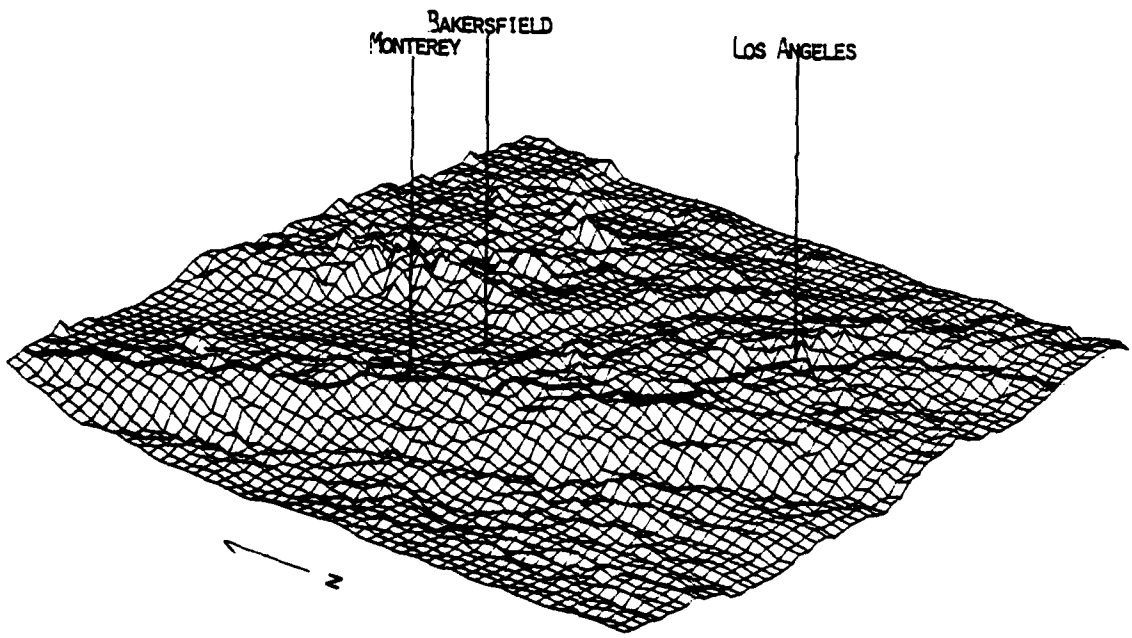

Figure 12. Topography 18 million years before present

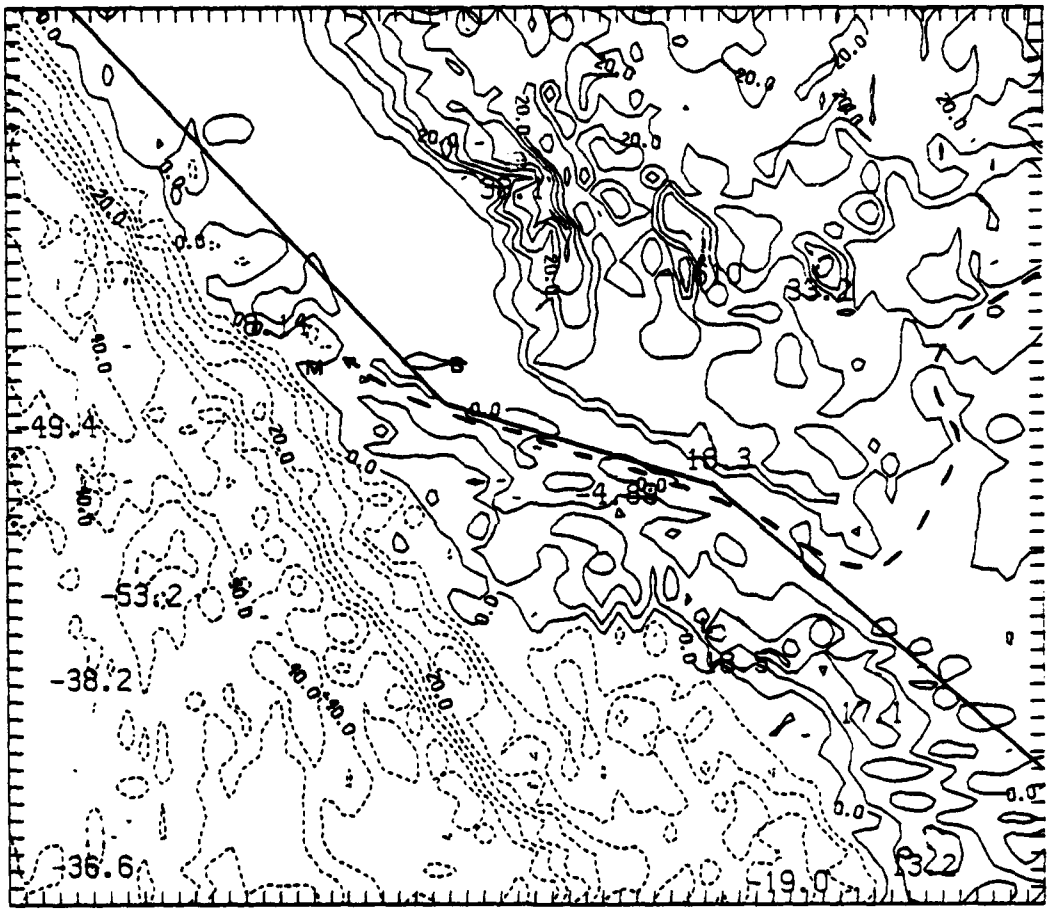

Figure 13. Eighteen million years before present, contour interval = 500 m, figures in hundreds of meters

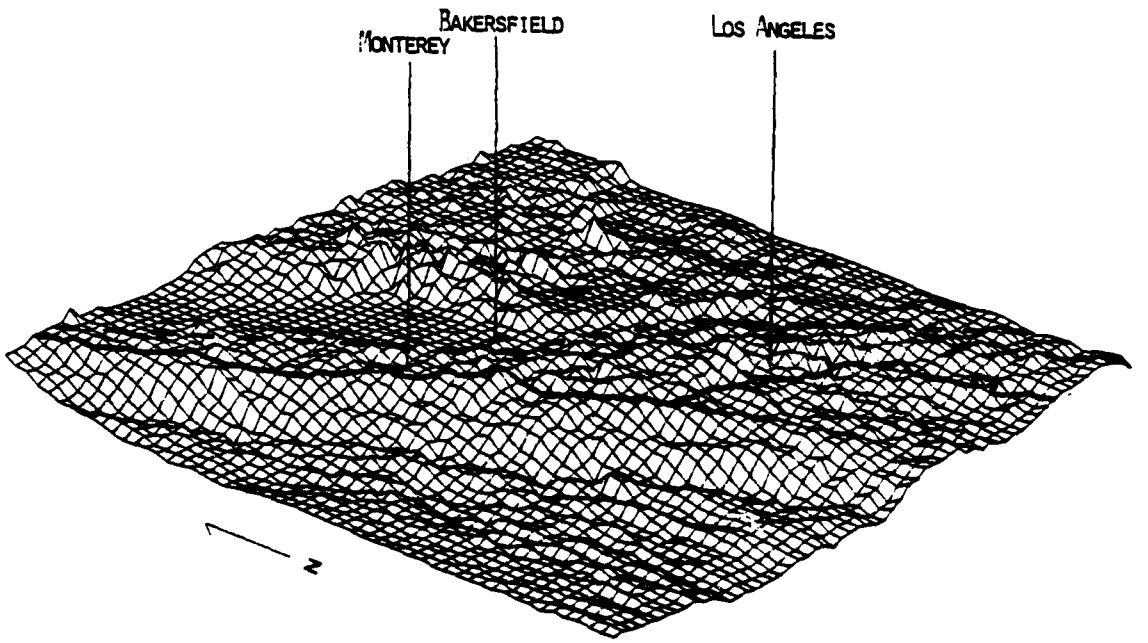

Figure 14. Topography 15 million years before present

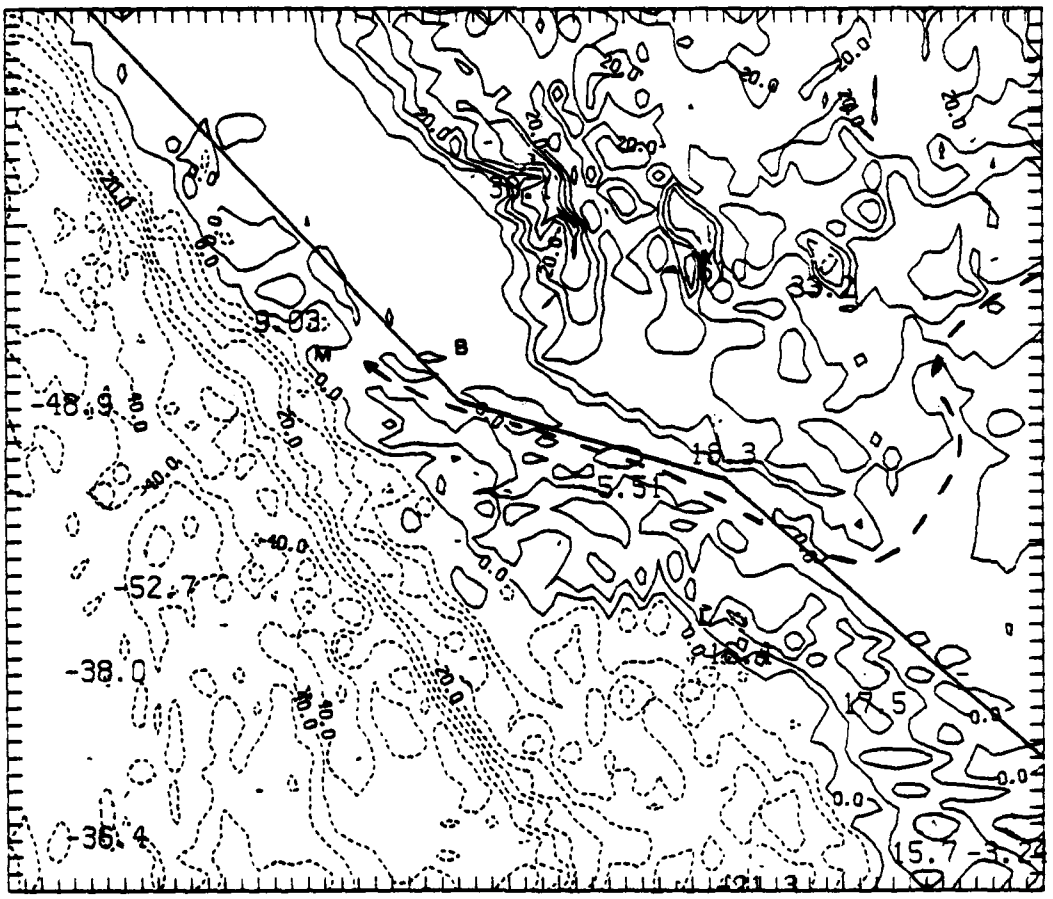

Figure 15. Fifteen million years before present, contour interval = 500 m, figures in hundreds of meters

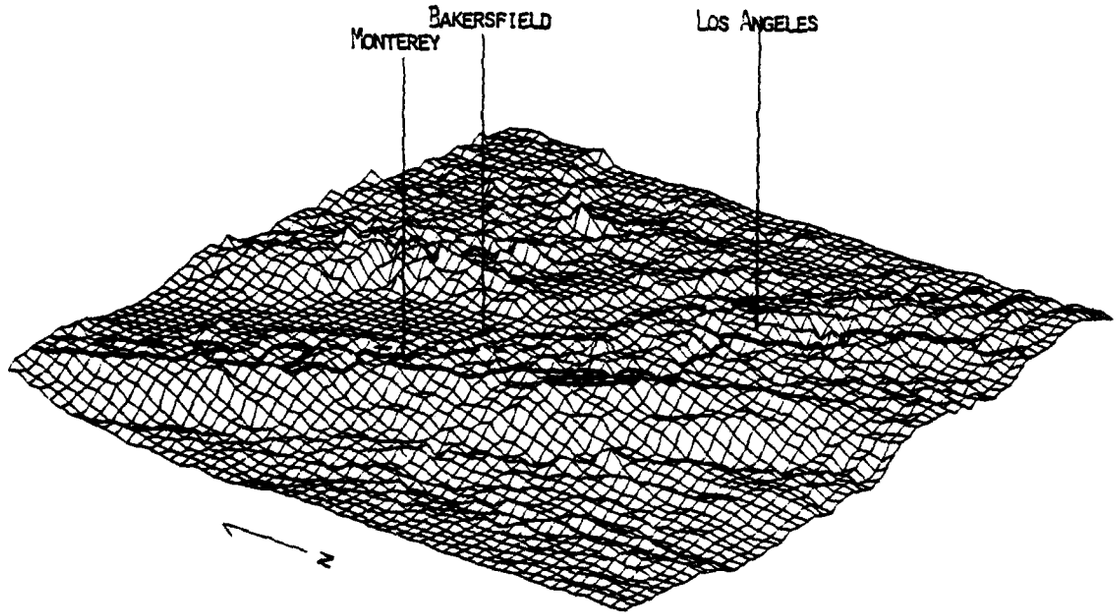

Figure 16. Topography 12 million years before present

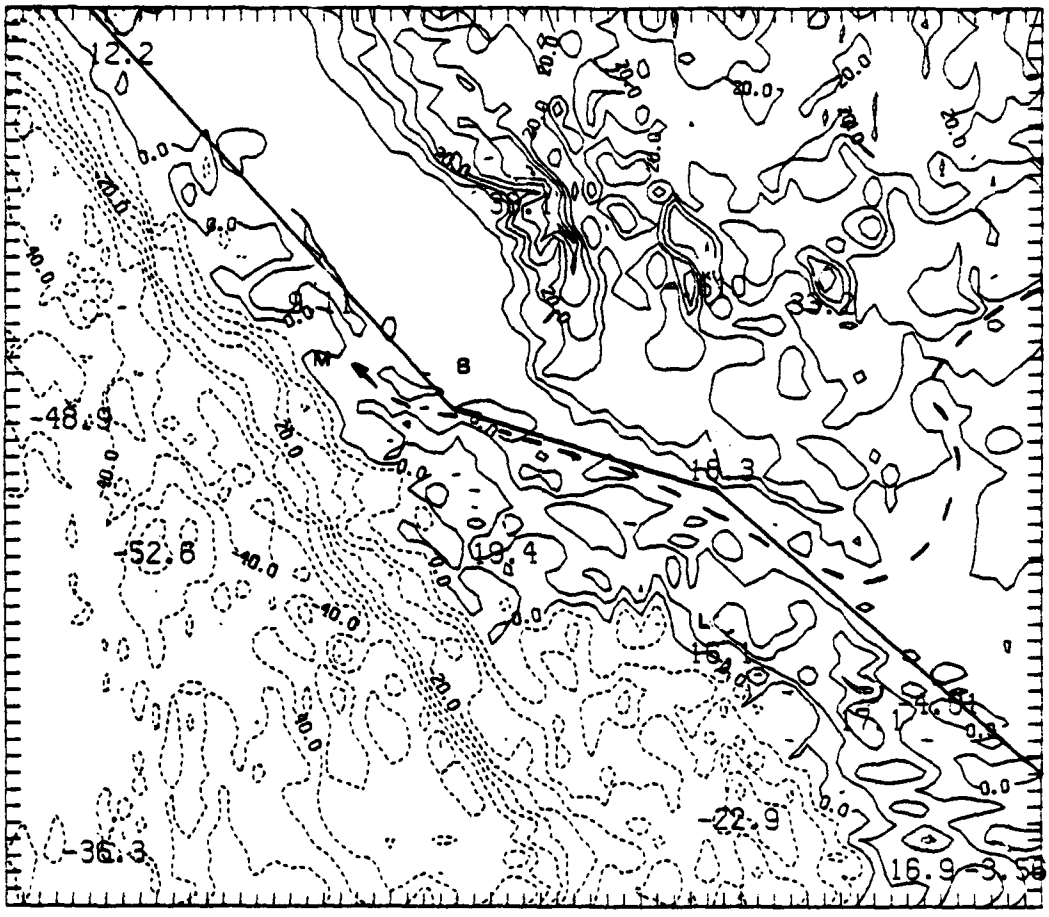

Figure 17. Twelve million years before present, contour interval = 500 m, figures in hundreds of meters

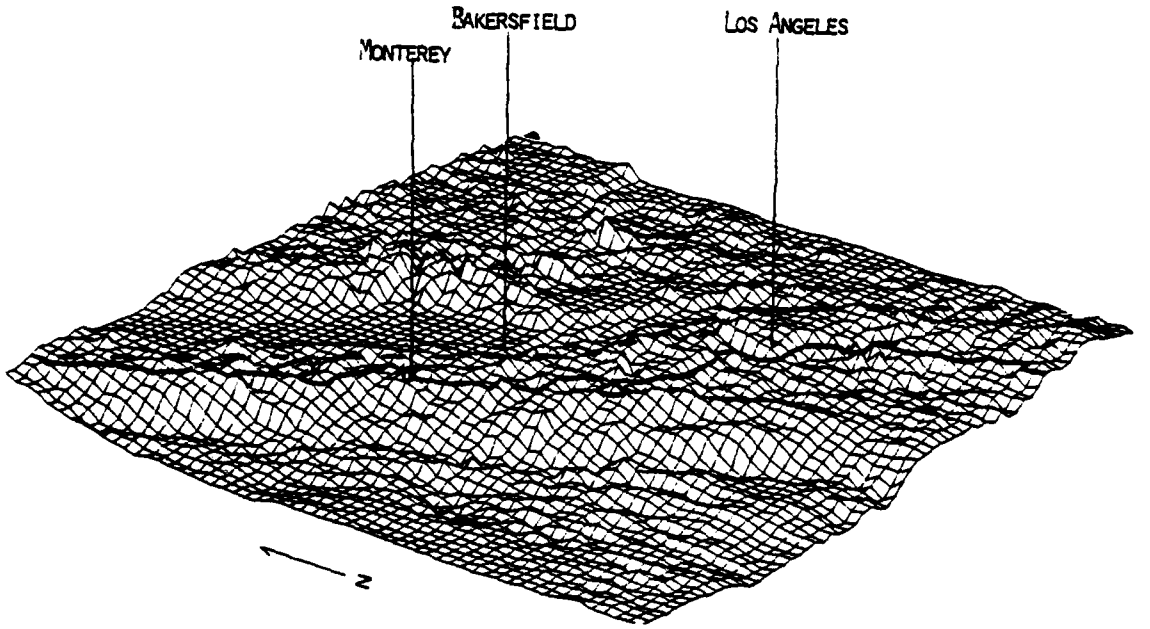

Figure 18. Topography 9 million years before present

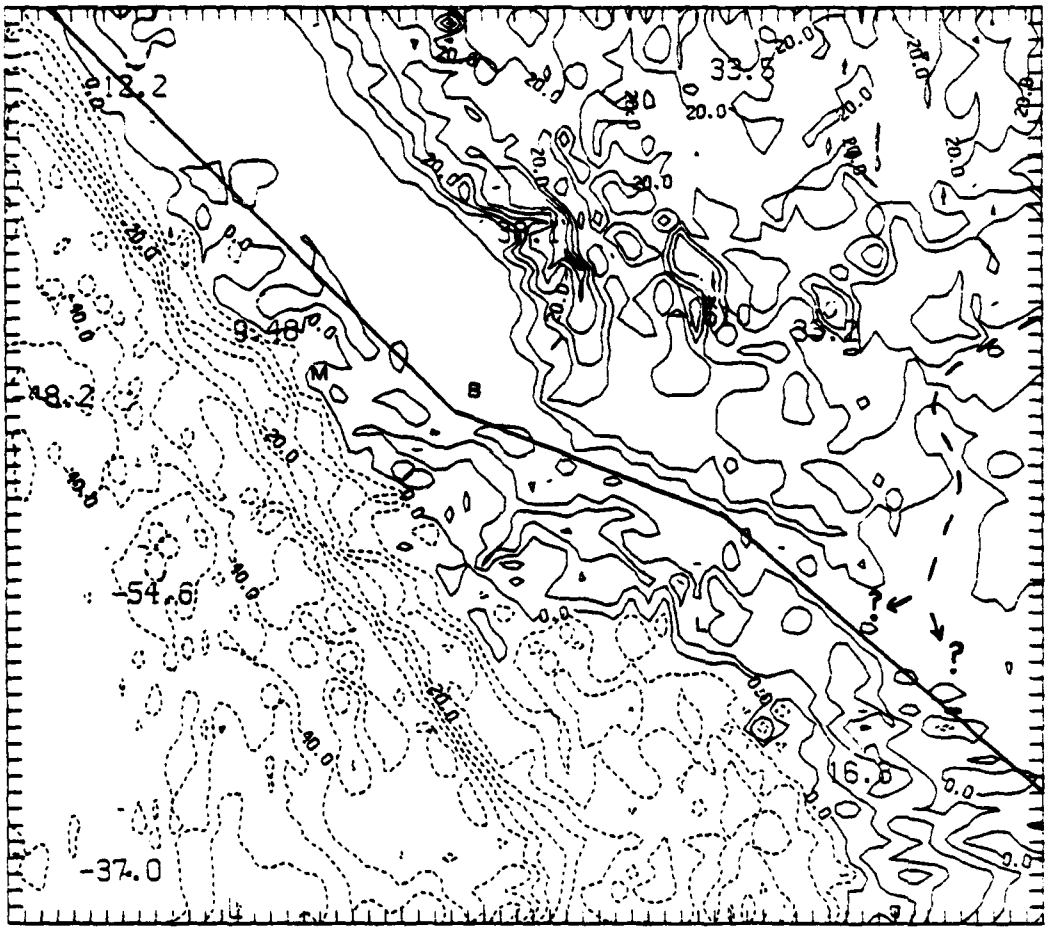

Figure 19. Nine million years before present, contour interval = 500 m, figures in hundreds of meters

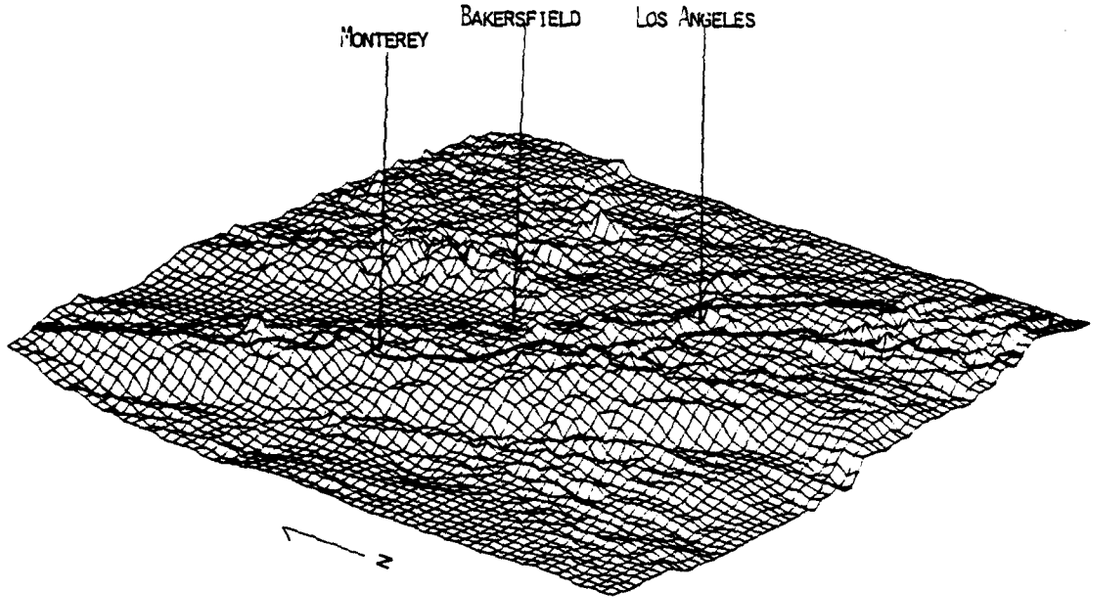

Figure 20. Topography 6 million years before present

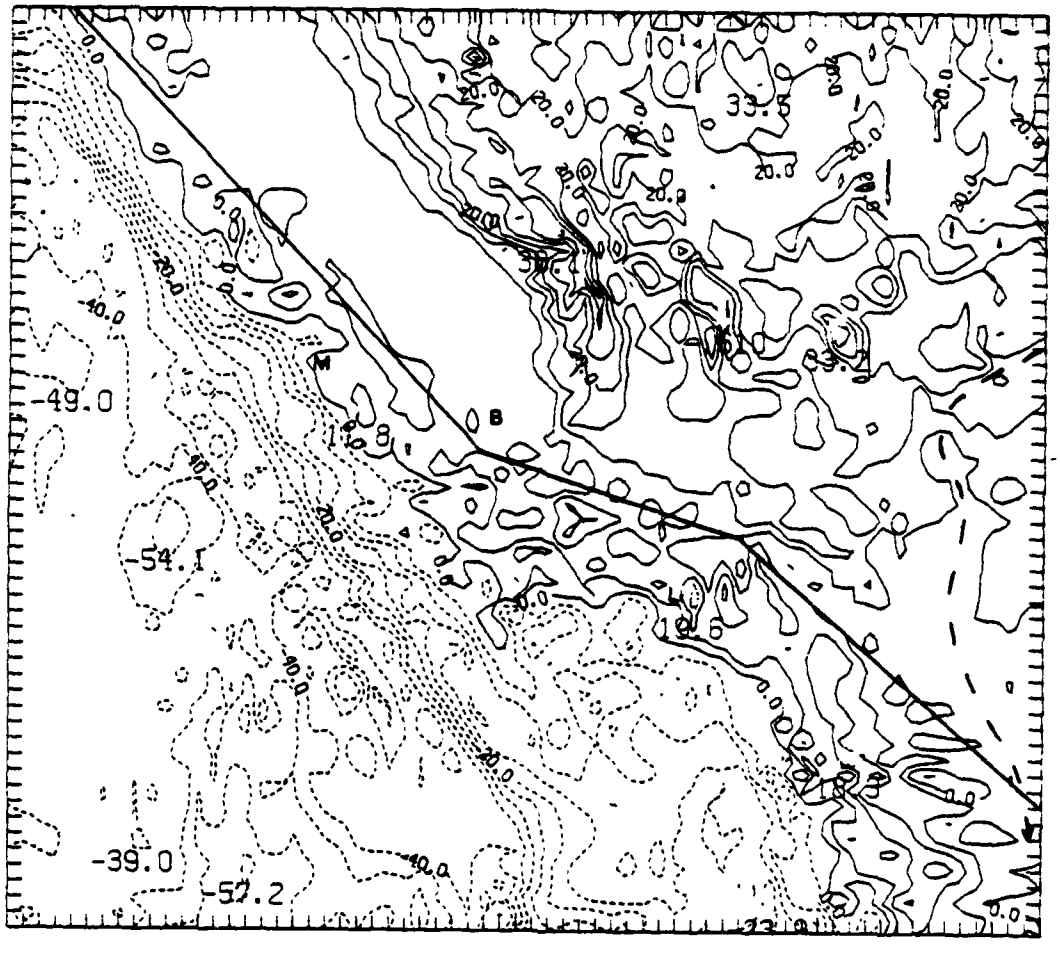

Figure 21. Six million years before present, contour interval = 500 m, figures in hundreds of meters

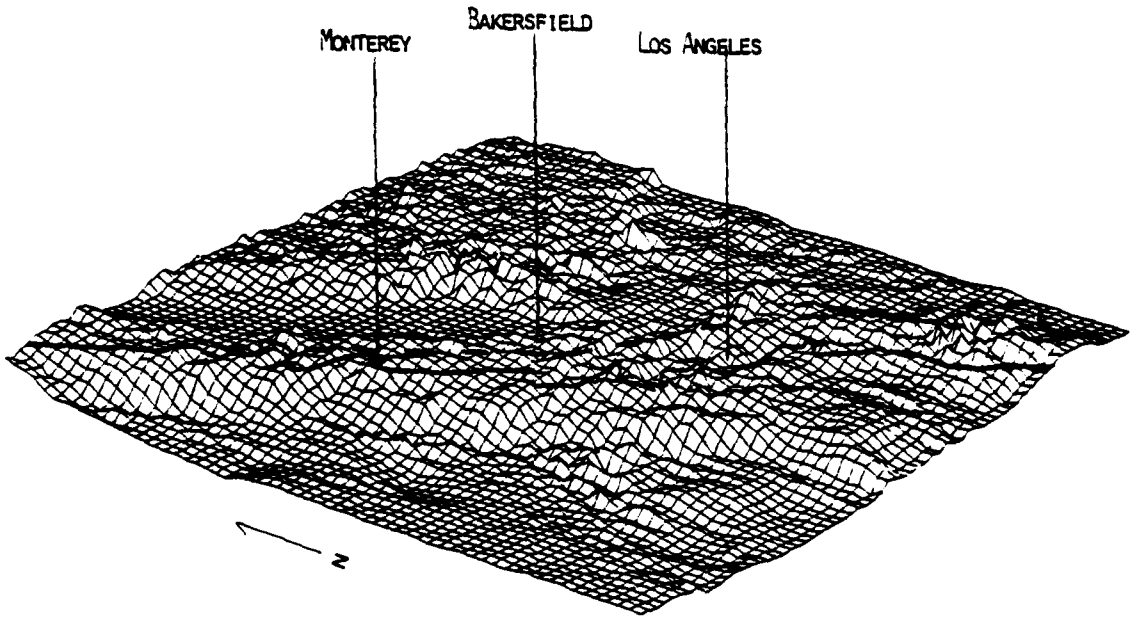

Figure 22. Topography 3 million years before present

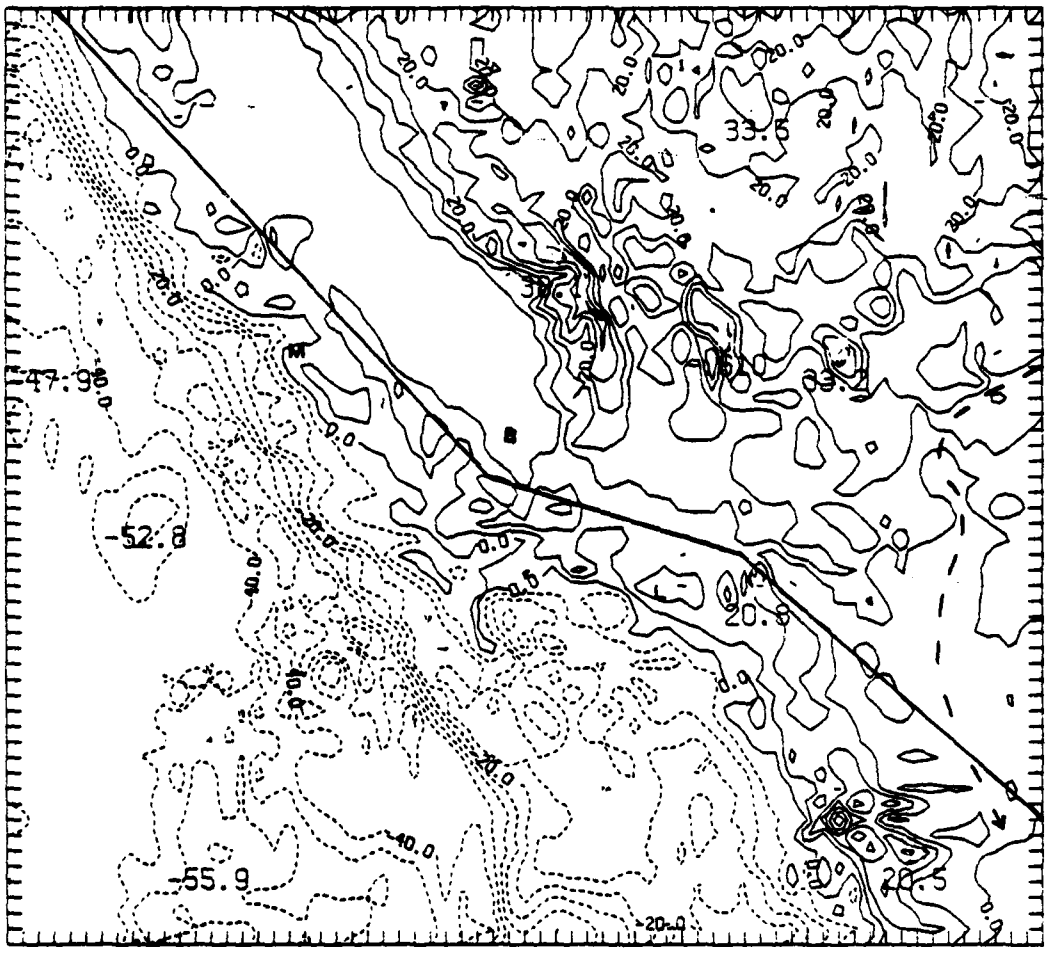

Figure 23. Three million years before present, contour interval = 500 m, figures in hundreds of meters

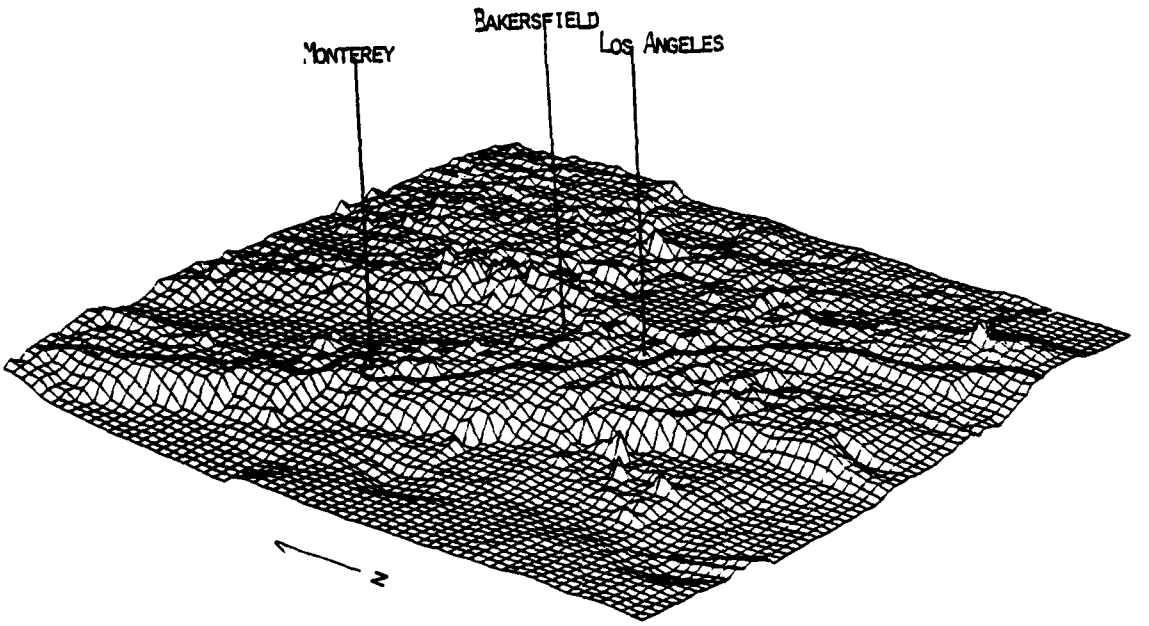

Figure 24. Present day topography

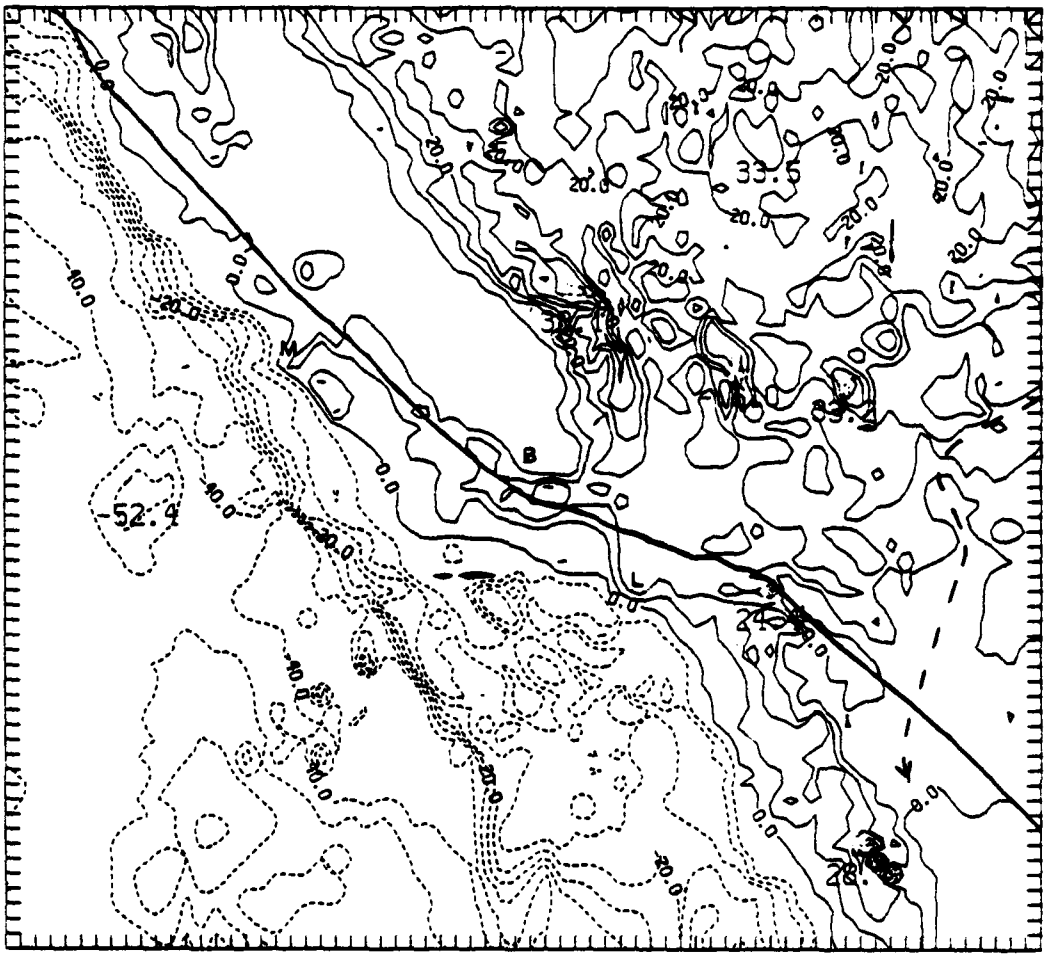

Figure 25. Present day, contour interval = 500 m, figures in hundreds of meters

III. RESULTS

In viewing the figures depicting model reconstructions of paleotopography, the design of the model must be kept in mind. Coarse resolution, as well as the simplifying assumptions of the model limit the scope of consideration to large scale effects.

Figures 10-25 are model outputs generated at three million year intervals. At each interval there is a three-dimensional topographic display and a contour map, both constructed from model results for that particular time. In all three-dimensional plots, the coastline (based on present sea level) is represented by a heavy solid line. The points corresponding to the cities of Monterey, Bakersfield, and Los Angeles have been annotated for reference.

All contour maps are oriented with north at the top. Bathymetry appears as dashed contours while all contours ≥ 0 appear as solid lines. The San Andreas Fault is represented as a heavy solid line. Inferred drainage patterns are indicated by a heavy dashed line. The points corresponding to the cities of Monterey, Bakersfield, and Los Angeles are labelled M, B, and L respectively.

Although the model runs backward in time, this discussion will start with model output at 21 million years before present and proceed foward in time for simplicity. As

output for each time interval is discussed, reference will be made to both figures (3-D and contour) representing output for that interval.

As expected, topography at 21 million years before present (Figures 10 and 11) differs greatly from present-day topography. Monterey Bay lies far to the south-east of its present position, approximately 100 km west of Bakersfield. Bakersfield, and points to the east of the San Andreas Fault, appear much as they are today. The Great Valley of California extends northwest of Bakersfield and is bounded on the east by the Sierra Nevada Mountains. The Mojave Desert lies to the south of the Sierra Nevadas. Along the fault itself, topography is depressed, particularly in the area to the southwest of the Mojave Desert. Areas to the west of the fault appear radically different than they do today. All topographic features which correlate to today's topography appear far to the southeast of their present positions. Although the general shape of the coastline and the mountain ranges are recognizable, they appear different than they do today. Monterey and San Francisco Bays are different in shape and location but are easily recognizable. The Coast Ranges to the north appear at lower elevations than they do today but are not greatly different in the area to the south of Monterey. The Transverse Ranges are somewhat lower and they are located to the southeast of their present positions as are the Peninsular Ranges. The position of the Peninsular

Ranges correlates geographically with the present-day position of the Gulf of California.

Despite the fact that this reconstruction is the product of a relatively simple geological model which does not take into account the effects of erosion, deposition, or displacements along other faults, the large scale features which appear in these figures are supported by geologic evidence. The Sierra Nevada Mountains (Curtis et al., 1958) and the Colorado Plateau (Eardley, 1962) are features which came into existence long before Miocene time. Also, the Gulf of California did not exist at this time (Larson et al., 1968; Larson, 1971; Van Andel and Shor, 1964). The depressed areas along the fault southwest of the Mojave Desert correlate geographically with the Salinas, Caliente, San Joacquin, Ridge, and Soledad basins. The geologic history of these basins (Norris and Webb, 1976; Blake et al., 1978) also shows good chronological correlation with the model reconstruction.

It is apparent from Figures 10 and 11 that drainage patterns were much different in early Miocene time. Drainage from the Colorado Plateau (Colorado River) could not flow southward into the Gulf of California as it does today. Rather this drainage flowed westward and entered the ocean somewhere to the north of the Transverse Ranges. Exactly where the terminus of this drainage system was located can

not be determined from model results alone. However, evidence previously presented indicates that Monterey Bay was the terminus of a major land drainage system at this time (Greene, 1977). The inferred drainage is illustrated in Figure 11. How long this drainage pattern had been in existence prior to early Miocene time is a question beyond the scope of this study. However, insights into changes which have occurred since early Miocene may be obtained by examining model output at intervals over the last 21 million years.

As expected from the relatively low velocity of motion along the fault from 21 million years before present to 10 million years before present (Table II), there is little change in topography over this period (Figures 10-17). It appears that the drainage pattern previously established would have been preserved over this interval. Although there is evidence to indicate that Monterey Submarine Canyon was filled and re-excavated during this time (Greene, 1977), this could have been the result of sea level fluctuations and does not necessarily imply large scale changes in land drainage patterns.

From 10-4.5 million years before present, motion along the fault increased in speed and became slightly less compressional in azimuth (Tables I and II, Figure 6). Topography at 9 million years before present (Figures 18 and 19) shows that compression along the fault in the area southwest of the

Mojave Desert is closing the depressions in that area. At the same time, the Peninsular Ranges have been moving northwestward, leaving a depressed area in the southeastern corner of the grid. At this point it is not possible to determine drainage patterns, as illustrated in Figure 19. At 6 million years before present (Figures 20 and 21), it is clear that compressional motion along the fault has uplifted the area to the southwest of the Mojave Desert to such an extent that this area no longer serves as a conduit for drainage. Simultaneously, the depressed area in the southeast corner has expanded due to continued movement of the Peninsular Ranges out of this area. It is not possible to determine that drainage actually flowed southward at this point since topography beyond the southeastern corner of the grid is not presented. However, geologic evidence (Larson et al., 1968; Larson, 1971) indicates that the Gulf of California developed at about this time. For this reason, it is assumed that drainage from the Colorado Plateau flowed southward much as it does today.

Velocity of relative motion is slightly higher over the last 4.5 million years to the present (Table II) and there is a slight change in the azimuth of direction (Table I and Figure 5). However, the trends concerning drainage continue during this interval as depicted in Figures 22-25. Northwestward displacement of points to the west of the San

Andreas Fault, compression in the area of the Transverse Ranges, and expansion of the Gulf of California continue to the present and are continuing today.

IV. CONCLUSIONS

In arriving at conclusions based on the results of a numerical model, care must be taken to consider the inherent weaknesses of the model and to examine available evidence from other sources for verification. In presenting model results, only large scale features and general trends were discussed. It is clear, from the description of the model, that these are the limits of its credibility. However, within these limits, model results correlate well with available evidence and indicate that the Colorado River was the erosional force involved in the excavation of Monterey Canyon.

LITERATURE CITED

Atwater, T. and Molnar, P., 1973, "Relative Motion of the Pacific and North American Plates Deduced from Sea-Floor Spreading in the Atlantic, Indian, and South Pacific Oceans," Proceedings of the Conference on Tectonic Problems of the San Andreas Fault System, Stanford University Publications, Geological Sciences, Volume XIII.

Blake, M. C. Jr., Campbell, R. H., Dibblee, T. W. Jr., Howell, D. G., Nilsen, T. H., Normark, W. R., Vedder, J. C., Silver, E. A., 1978, "Neogene Basin Formation in Relation to Plate Tectonic Evolution of San Andreas Fault System, California," The American Association of Petroleum Geologists Bulletin, V. 62, No. 3, pp. 344-372, March.

Clark, J. C. and Rietman, J. D., 1973, United States Department of the Interior Geological Survey Prof. Paper 783, Oligocene Stratigraphy, Tectonics, and Paleogeography Southwest of the San Andreas Fault, Santa Cruz Mountains and Gabilan Range, California Coast Ranges.

Courant, R., K. O. Friedrichs, and H. Lewy, 1928, "Uber die partiellen differenzengleichungen der mathematischen physik," Math. Annalen, 100, 32-74.

Crowell, J. C., 1962, Displacement Along the San Andreas Fault, California, The Geological Society of America.

Curtis, G. H., Evernden, J. F., and Lipson, J., 1958, "Age Determination of Some Granitic Rocks in California by the Potassium-argon Method," Dept. Nat. Resources Div. Mines Special Report. 54.

Eardley, A. J., 1962, Structural Geology of North America, pp. 295-301, Harper and Row.

Greene, H. G., 1977, United States Department of the Interior Geological Survey Open-File Report 77-718, Geology of the Monterey Bay Region.

Haltiner, G. J., and Williams, R. T., 1980, Numerical Prediction and Dynamic Meteorology, pp. 130-132, John Wiley and Sons, Inc.

Larson, R. L., 1971, "Near Bottom Geologic Studies of the East Pacific Rise Crest," Geol. Soc. Amer. Bull., V. 82, pp. 823-842.

Larson, R. L., Menard, H. W., and Smith, S. M., 1968, "Gulf of California: A Result of Ocean Floor Spreading and Transform Faulting," Science, V. 161, pp. 781-784.

Martin, B. D. and Emery, K. O., 1967, "Geology of Monterey Canyon, California," The American Association of Petroleum Geologists Bulletin, V. 51, No. 11, pp. 2281-2304, November.

Menard, H. W., 1960, "Possible Pre-Pleistocene Deep-Sea Fans off Central California," Geological Society of America Bulletin, V. 71, pp. 1271-1278.

Norris, R. M. and Webb, R. W., 1976, Geology of California, pp. 123-134, John Wiley and Sons, Inc.

Silver, E. A., McCulloch, D. S., and Curray, J. R., "Marine Geology and Tectonic History of the Central California Continental Margin." Unpublished.

Starke, G. W. and Howard, A. D., 1968, "Polygenetic Origin of Monterey Submarine Canyon," Geological Society of America Bulletin, V. 79, No. 7, pp. 813-826.

van Andel, Tj. H., and Shor, G. G., eds., 1964, Marine Geology of the Gulf of California, Amer. Assoc. Petrol. Geologists.

LIST OF REFERENCES

Bonnin, J., Francheteau, J., and Le Pichon, X., Plate Tectonics, Elsevier Scientific Publishing Company, 1973.

California Division of Mines and Geology Special Report 118, San Andreas Fault in Southern California, edited by J. C. Crowell, 1975.

Dickinson, W. R. and Grantz, A., eds., Proceedings of Conference on Geologic Problems of San Andreas Fault System, Stanford University, 1968.

Eardley, A. J., Structural Geology of North America, Harper and Row, 1962.

Kovach, R. L. and Nur, A., eds., Proceedings of Conference on Tectonic Problems of San Andreas Fault System, Stanford University, 1973.

Norris, R. M. and Webb, R. W., Geology of California, John Wiley and Sons, Inc., 1976.

Shepard, F. P., Submarine Topography off the California Coast, Geological Society of America, 1941.

Shepard, F. P., Submarine Geology, Harper and Row, 1973.

Whitaker, J. H. McD., ed., Submarine Canyons and Deep-Sea Fans, Dowden, Hutchinson and Ross, Inc., 1976.

INITIAL DISTRIBUTION LIST

		No. Copies
1.	Defense Technical Information Center Cameron Station Alexandria, Virginia 22314	2
2.	Library, Code 0142 Naval Postgraduate School Monterey, CA 93940	2
3.	Chairman (Code 68 Mr) Department of Oceanography Naval Postgraduate School Monterey, CA 93940	1
4.	Chairman (Code 63 Rd) Department of Meteorology Naval Postgraduate School Monterey, CA 93940	1
5.	Dist. Prof. E. C. Haderlie, Code 68 Hc Department of Oceanography Naval Postgraduate School Monterey, CA 93940	1
6.	LT Robert L. Allen, Jr. 118 Moran Circle Monterey, CA 93940	1
7.	Director Naval Oceanography Division Naval Observatory 34th and Massachusetts Avenue NW Washington, D. C. 20390	1
8.	Commander Naval Oceanography Command NSTL Station Bay St. Louis, MS 39522	1
9.	Commanding Officer Naval Oceanographic Office NSTL Station Bay St. Louis, MS 39522	1

10. Commanding Officer — 1
Fleet Numerical Oceanography Center
Monterey, CA 93940

11. Commanding Officer — 1
Naval Ocean Research and Development Activity
NSTL Station
Bay St. Louis, MS 39522

12. Commanding Officer — 1
Naval Environmental Prediction Research Facility
Monterey, CA 93940

13. Chairman, Oceanography Department — 1
U. S. Naval Academy
Annapolis, MD 21402

14. Chief of Naval Research — 1
800 N. Quincy Street
Arlington, VA 22217

15. Office of Naval Research (Code 420) — 1
Naval Ocean Research and Development Activity
NSTL Station
Bay St. Louis, MS 39522

16. Scientific Liaison Office — 1
Office of Naval Research
Scripps Institution of Oceanography
La Jolla, CA 92037

17. Library — 1
Scripps Institution of Oceanography
La Jolla, CA 92037

18. Library — 1
Department of Oceanography
University of Washington
Seattle, WA 98105

19. Library — 1
CICESE
P. O. Box 4803
San Ysidro, CA 92073

20. Librarian — 1
Hopkins Marine Station
Pacific Grove, CA 93950

21. Library 1
School of Oceanography
Oregon State University
Corvallis, OR 97331

22. Commander 1
Oceanographic Systems Pacific
Box 1390
Pearl Harbor, HI 96860

23. Chief, Ocean Services Division 1
National Oceanic and Atmospheric
Administration
8060 Thirteenth Street
Silver Springs, MD 20910

24. Dr. H. G. Greene 1
U. S. Geological Survey
Branch of Pacific-Arctic Marine Geology
345 Middlefield Road, MS-99
Menlo Park, CA 94025

25. Dr. F. P. Shepard 1
Scripps Institution of Oceanography
La Jolla, CA 92037

26. Dr. R. F. Dill 1
Scripps Institution of Oceanography
La Jolla, CA 92037

27. Prof. R. T. Williams, Code 63Wu 1
Meteorology Department
Naval Postgraduate School
Monterey, CA 93940

28. Mrs. Betty W. Allen 1
2453-D Amsterdam Circle
Marietta, GA 30067

29. Capt. Alan Shaffer 1
Meteorology Department, Code 63
Naval Postgraduate School
Monterey, CA 93940

30. Mr. J. R. MacFarlane 1
1819 Applewood Court
Orlando, FL 32808

31. Librarian 1
Moss Landing Marine Laboratory
Moss Landing, CA 95039